IRAQI JOURNAL OF APPLIED PHYSICS
Vol. (14), No. (3), July-September 2018, pp. 41-45

Synchrotron-Radiation Infrared Microscopy Analysis of an Amyloid Peptide Irradiated by Mid-Infrared Free-Electron Laser

Maisun R. Elewi

College of Engineering,
Muthanna University,
Samawa City,
Muthanna Province, IRAQ

In this work, we have irradiated amyloid fibrils with a free-electron laser (FEL) tuned to mid-infrared frequencies to induce dissociation of the aggregates into monomer forms. Synchrotron-radiation infrared microscopy (SR-IRM) is a powerful tool for in situ analysis of minute structural changes of various materials, and in this study, the feasibility of SR-IRM for analyzing the microscopic conformational changes of amyloid fibrils of a peptide after FEL irradiation was investigated. Reflection spectra of the amyloid fibril surface showed that the amide I peaks shifted to higher wavenumbers after the FEL irradiation, indicating that the initial β-sheet-rich structure transformed into a mixture of non-ordered and turn-like peptide conformations. This result demonstrates that conformational changes of the fibril structure after the FEL irradiation can be observed at a high spatial resolution using SR-IRM analysis and the FEL irradiation system can be useful for dissociation of amyloid aggregates.

Keywords: Infrared Microscopy Analysis; Amyloid Peptide; Free-Electron Laser; Synchrotron-radiation
Received: 4 June 2018, **Revised:** 25 July 2018; **Accepted**: 1 August 2018

1. Introduction

Over the last three decades, photodynamic therapy (PDT) has become a useful clinical tool and a viable alternative to other established therapies in the treatment of cancer and other diseases. In fact, PDT has potential application to a wide variety of cancers, including lung, cervical, esophageal, gastric, and breast carcinoma [1,2]. In dermatology, PDT is considered for the treatment of basal cell carcinoma, actinic keratoses, cutaneous lesions of Bowen's disease, psoriasis, cutaneous T-cell lymphoma, acne, and more recently it has been proposed for photo-rejuvenation [3,4]. The advantages in this field include the capacity for non-invasive targeted therapy (*via* the topical application of the drug and local irradiation of involved areas) as well as the ability to generate excellent cosmetic results with minimal discomfort. In ophthalmology, the recent application of Verteporfin for the PDT of age-related macular degeneration (AMD) represented the first breakthrough in the use of PDT to treat an otherwise untreatable condition [4].

Several disciplines have contributed to the development of PDT: chemistry, in the identification and preparation of new photosensitizing agents (photosensitizers, PS); biology, in the elucidation of the cellular processes involved in PDT; pharmacology and physiology, in identifying the mechanisms of distribution of PS in an organism; and last but not least physics, in the construction of suitable light sources, imaging devices and optical sensors, and in the development of dosimetric concepts and spectroscopic methods for determining PS concentrations in different cells and tissues. Biophysics have also helped to focus on the role of pH for PS accumulation, dose rate effects, oxygen depletion, temperature, and optical penetration of light at different wavelengths into various types of tissue: these are all important factors to be taken into account to optimize the effects of PDT [6].

Essentially, PDT involves the administration of a PS, which selectively accumulates in target cells, followed by exposure of the cells to a light source. Excitation of the PS molecules with light generates reacting species leading to oxidative damage of cellular structures. The photochemical reaction is described by the Jablonski diagram (Fig. 1). The ground electronic state of the PS is a singlet state (S_0). On absorption of light of appropriate wavelengths (1), the PS is excited to the short-lived first excited singlet-state (S_1), from which it can return to the S_0-state by emitting the absorbed energy as fluorescence (2) or by internal conversion (3). Alternatively, the S_1 PS can convert to the first excited triplet state (T_1) by intersystem crossing (4). The loss of energy from T_1 to the S_0-state can occur by emitting a phosphorescence photon (5). However, the T_1-state is sufficiently long-lived to favor the interaction of the excited PS with the surrounding molecules, with the generation of cytotoxic species (6). Therefore the photodynamic action is mostly mediated by the T_1-state.

Amyloidosis is caused by the deposition of amyloid fibrils in various organs of a mammalian body [7-9]. A common form of amyloidosis, Alzheimer's disease, is becoming more common as the population increases [10]. Furthermore, cancer-associated diseases such as multiple myeloma are

caused by amyloidosis, and an effective therapy for the amyloidosis has not yet been developed [11]. Amyloid fibrils are recognized as a clinical target, and they have a common secondary structure, cross-β structure, that is formed by peptides and various proteins [9]. Decreasing the amount of amyloid fibrils in tissues is considered to be an effective treatment for amyloidosis, but it is difficult to dissociate the robust fibril structure unless organic solvents or synthetic molecules are used [12,13].

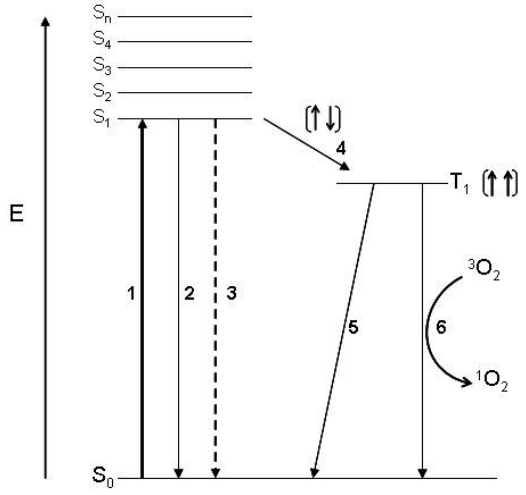

Fig. (1) Modified Jablonski diagram. Photophysical processes: 1-absorption, 2-fluorescence, 3-internal conversion, 4-intersystem crossing, 5-phosphorescence and 6-formation of singlet oxygen $^1O_2$ by energy transfer from T1 photosensitizer to triplet oxygen $^3O_2$

We have recently found that a free-electron laser (FEL) tuned to the amide I band (1600–1700 cm^{-1}) is able to dissociate the amyloid fibrils of lysozyme and of a five-residue peptide (DFNKF) of the thyroid hormone [14,15]. In the case of lysozyme fibrils, the β-sheet content of the fibrils diminishes, and the enzyme can be refolded into the active form after the FEL irradiation [14]. FEL can deliver picosecond pulses, high-photon density, and high-power radiation [16-20], and it can be suggested that non-covalent bonds such as hydrogen bonds between the β-sheet structures of amyloid fibrils are cleaved by the high-powered pulsed laser tuned to the frequency of amide C=O stretching vibration to induce the disaggregation of amyloid fibrils [14]. The structural change was determined using conventional Fourier transform infrared (FTIR) spectroscopy in the previous study. In the case of the short peptide, however, FTIR spectroscopy could not determine the conformational changes in detail because the peptide has several conformations and a flexible structure in solution [15]. X-ray crystallography and nuclear magnetic resonance (NMR) are usually employed to determine the structure of peptides [21-23], but while these analytical methods are excellent for three-dimensional structural determination at the atomic level, they are also time consuming, and once analyzed, samples cannot be re-used for other analytical methods. In contrast, IR absorption spectral measurements are comparatively simple, and the spectra are sensitive to the secondary structures of the peptides [24]. Moreover, the normal structure of a peptide can be easily distinguished from the amyloid fibril structure in IR spectra because a peak of the amide I band shifts to a smaller wavenumber as the content of β-sheet structure increases during fibrillation of the peptide [25,26]; IR absorption measurements are therefore also useful for detecting amyloid fibrils, as reviewed in a recent paper [27]. IR microscopy analysis is often employed for studying the local structure of organic materials and biomaterials [28,29], and its advantages lie in the fact that no labeling or pre-treatment of the sample is required, which means samples can be re-used. The use of synchrotron radiation in combination with IR microscopy analysis improves the spatial resolution with a high signal-to-noise (S/N) ratio compared to that using a thermal radiation beam because high-power light can be delivered to a small area in a small sample (of several micrometers section) [30]. Synchrotron radiation IR microscopy (SR-IRM) has recently been used for monitoring the protein secondary structures of silk and investigating protein phosphorylation in living cells [31,32]. Encouraged by these studies, we investigated the use of SR-IRM for detecting the minute (conformational) structural changes of amyloid fibrils formed by a short peptide after irradiation with an FEL tuned to the amide I band.

2. Experimental Part

All of the reagents used in this study were purchased as special-grade chemicals. Tris-base, dimethyl sulfoxide (DMSO), hydrochloric acid, and sodium chloride were purchased from Wako Pure Chemical Industries (Osaka, Japan); synthesized pentapeptide, DFNKF (80.9% purity), from PH Japan Co., Ltd. (Hiroshima, Japan).

The thyroid hormone pentapeptide, DFNKF, was dissolved in 10% DMSO in buffer A, which contained 10mM of tris-base and 20mM of NaCl; the pH of the solution was adjusted to 7.5 using HCl. The peptide powder was dissolved at a concentration of 100mg/mL in DMSO and then diluted to 10 mg/mL using buffer A. The solution was incubated for two days at 37°C, after which 100μL of the solution containing amyloid fibrils was placed on a stainless-steel substrate (Jasco International Co., Ltd., Tokyo, Japan) and irradiated with the FEL beam (tuned to the amide I band) at 37°C. To prevent water evaporation, 10μL of water was added periodically to the suspension during irradiation. After irradiation, the sample on the substrate was air-dried before IR absorption measurements were performed.

The FEL-TUS uses synchrotron radiation (SR) as a seed to generate a laser beam with a variable wavelength in the mid-infrared region (5.0-16μm; 625-2000cm^{-1}) (Fig. 2) [20]. An electron beam generated by a high-radio-frequency (RF) electron gun (2.856GHz) is accelerated to a maximum energy of 40 MeV by a linear accelerator and injected into an undulator (a periodic magnetic field). The oscillations of the electron beam in the undulator generate SR. The maximum value of the periodic magnetic flux density is set to 0.83 T, and the amplified SR is reflected upstream of the electron beam by a mirror positioned downstream of the beam, and then re-reflected by the upstream mirror to interact with the electron beam again, producing coherent laser light.

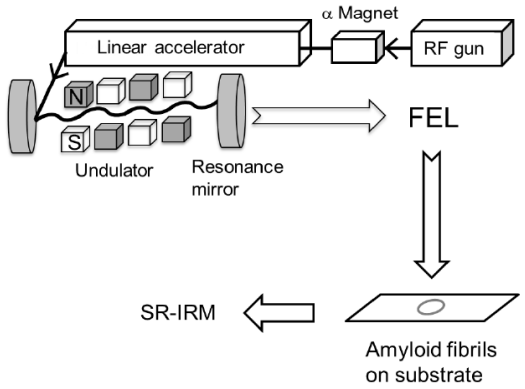

Fig. (2) Schematic of the FEL and analysis setup. The laser beam is generated using an electronic gun and accelerated to 40 MeV by the linear accelerator. The periodic length of the undulator can be tuned to set the oscillation wavelength. The FEL beam is transported to the laboratory though a vacuum tube, and the irradiation to the sample on the substrate is controlled by a gold-coated mirror. After irradiation, the sample was analyzed using SR-IRM

The FEL-TUS provides two types of laser pulses: macro- and micropulses. Macropulses have duration of ~2μs and a repetition rate of 5 Hz during operation; the macropulses consists of a train of 2-ps micropulses separated by an interval of 350ps. The energy of each laser macropulse used for the current experiment was in the range of 6.0-8.0 mJ, as measured using an energy meter (SOLO2, Gentec-EO Inc., Quebec, Canada). Prior to the irradiation, the beam was focused to a point above the sample using a He-Ne beam. The spot size of beam line was ca. 0.5 cm in diameter.

The SR-IR microscopic analysis was performed using the IR micro-spectroscopy beam line (SRMS, BL-15) at the SR center of Ritsumeikan University [33]. The beam line is equipped with Nicolet 6700 and Continuμm XL IR microscopes (Thermo Fisher Scientific Inc.). Measurements were performed in reflection mode with a 32× Cassegrain lens and a 10×10μm aperture. Spectra were collected in the mid-IR range of 700–4000cm^{-1} at a resolution of 4 cm^{-1} with 256 scans. Smoothing and normalization of spectra were performed on the amide I band (1600-1700cm^{-1}) by using Spectra Manager software Ver. 2 (Jasco International Co., Ltd., Tokyo, Japan).

3. Results and Discussion

We found that FEL irradiation of DFNKF amyloid fibrils caused disaggregation when the FEL light was tuned to the amide I band (6.08μ, *ca*.1644cm^{-1}) [15]. Since the peak intensity of the peptide increased after the fibrillation compared to the other peaks within amide I region (1600-1700cm^{-1}), we considered that the increase of the peak intensity reflected the β-sheet-rich fibril structure of the peptide. The surface area of the amyloid fibrils was analyzed using SR-IRM at several positions with 10×10μm square aperture (Fig. 3 and 4). Since the minimum size of fibrils bundle was estimated to be around 10 μm as indicated in a previous study [15], this aperture size was selected in this study. Spectra were collected from areas with a lighter contrast in the microscope image to suppress the background contribution in reflection mode (Fig. 3a and 4a). The positions for measurement were numbered in those images. A total of nine spectra were collected from the samples both before and after FEL irradiation over a wavenumber range of 1600–1700cm^{-1} (the amide I region). Almost of reflection spectra indicated that before FEL irradiation the amyloid fibrils had two major absorption bands: <1640cm^{-1} and around 1670cm^{-1} (Fig. 3b) and (c)). The former bands were ranged from 1635 to 1640 cm^{-1}, and the latter bands were from 1668 to 1670 cm^{-1}. This spectrum pattern having two major amide I bands is characteristic of the short peptide as indicated in the previous study [15] and distinct from that of large protein such as lysozyme which has single major amide I band [14]. This means that there are several conformations in the fibrils structure of the DFNKF peptide, that is anti-parallel β-sheet structures mixed with non-ordered structures and turns [27,34,35].

Although a possibility that the latter bands correspond to the amide side chain of asparagine (N) cannot be excluded, the absorbance of the amide backbone is probably strong in contrast to that of the side chain. These spectra imply that the almost the whole sample surface was covered with amyloid fibrils, although spectra from the entire area were not collected. On the contrary, the peaks in the SR-IR spectra around 1640 and 1670 cm^{-1} shifted to larger wavenumbers after FEL irradiation (Fig. 4b and c). Some spectra (no.1 and no. 4) exhibited peaks close to 1680 cm^{-1}. Moreover, both bands around 1640 and 1670 cm^{-1} had a width of about 30 cm^{-1} after the irradiation, while those had a width of about 20 cm^{-1} before the irradiation, that is the widths of amide I bands after the FEL irradiation were broad compared to those before the irradiation. These results indicate that there were fewer β-sheet structures and more non-ordered and turns structures in the local fibrils after FEL irradiation [27,35].

Although more concrete secondary conformations of peptides could not be determined by these analyses, the above results clearly indicate that the FEL irradiation is capable of disaggregating peptide amyloid fibrils and can produce substantially non-β-sheet peptides.

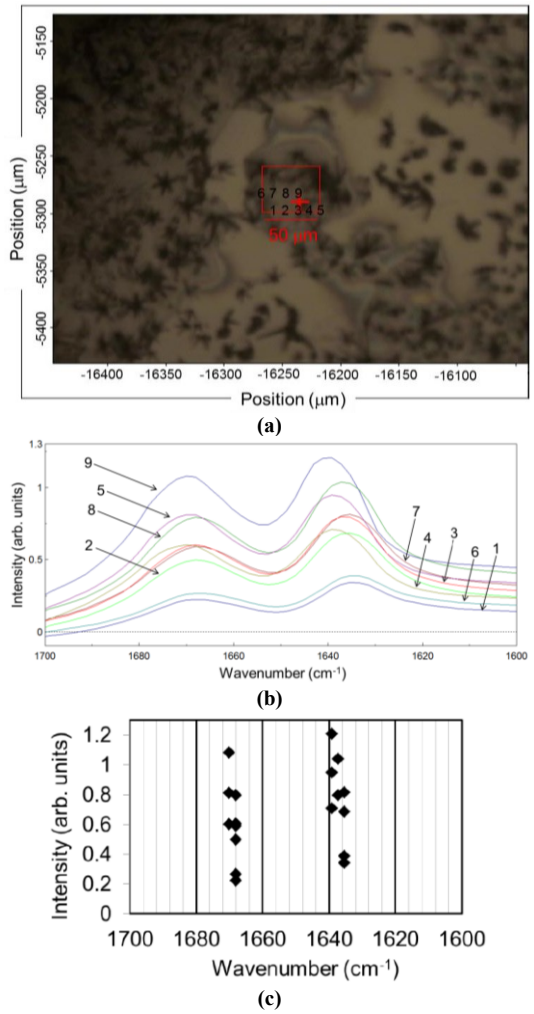

Fig. (3) (a) SR-IRM image of the DFNKF amyloid fibrils before FEL irradiation. The target size was 50×40μm. The numbers (no.1-9) indicate the positions for measurements of spectra. (b) IR reflection spectra. (c) Plot of the peaks in the amide I region

In our previous study, we measured the FTIR spectra of amyloid fibrils from lysozyme and DFNKF peptide after they had been mixed with KBr powder [14,15]. This meant that the sample could not be re-used, and we were unable to obtain any spatial information about the structural changes of the sample; however, the average structure influenced the spectrum. IR microscopy, in contrast, can reveal spectral information about the structural changes of the peptides without the need for labeling, and SR-IRM provides this information at a high spatial resolution.

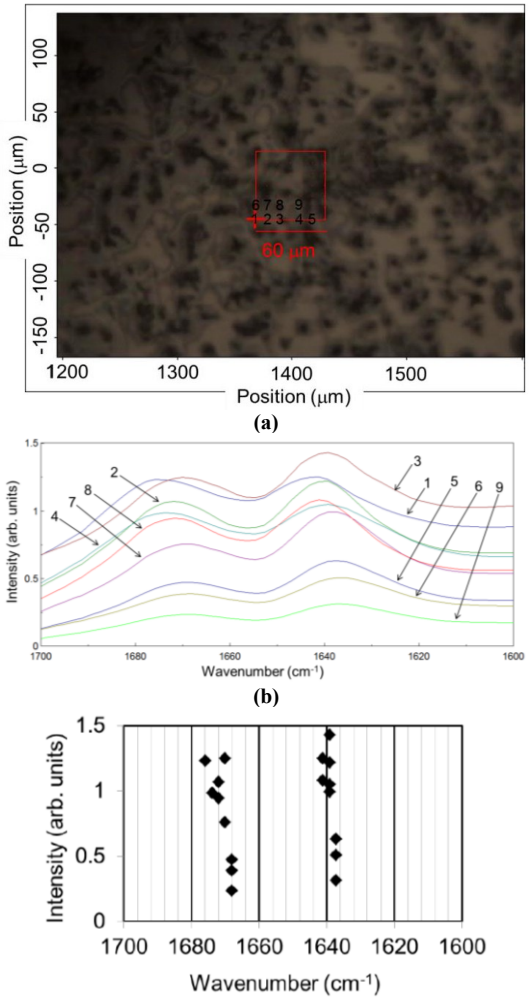

Fig. (4) (a) SR-IRM image of the DFNKF amyloid fibrils after FEL irradiation. The target size was 60×60 μm. The numbers (no. 1-9) indicate the positions for measurements of spectra, (b) IR reflection spectra, and (c) Plot of the peaks in the amide I region

For a pathological diagnosis of amyloidosis, it is necessary to be able to detect local amyloid-fibril deposition areas in tissues, and the results of this study indicates that there is a possibility that SR-IRM could be used for this purpose [27]. Moreover, the implication that there are various peptide conformations within a small area of amyloid fibrils after FEL irradiation suggests that FEL irradiation may be an effective tool for dissociating aggregated amyloid structures. The SR-IRM system can be regarded as suitable for detecting a small amount of amyloid fibrils in pathological tissues. Furthermore, the fact that the structural changes of the amyloid fibrils after FEL irradiation could be observed using SR-IRM means that this analytical system can be considered as a possible screening assay for inhibitors targeting amyloid fibrils [13]. For example, the inhibitory effect of candidate drugs on the dissociation of amyloid fibrils on the substrate could be tested using SR-IRM as shown in this study.

4. Conclusions

In conclusion, an FEL tuned to the amide I band was employed to irradiate peptide amyloid fibrils, and the structural changes of the fibrils were analyzed using SR-IRM. The results demonstrated that rigid fibril structures disaggregate under irradiation by an FEL beam and are converted to flexible peptide conformations. The FEL irradiation system will become an effective tool for dissociation of pathological amyloid aggregates.

References

[1] C. Hopper, Lancet Oncol., 1, 212-219 (2000).
[2] D.E. Dolmans, D. Fukumura and R.K. Jain, Nat. Rev. Cancer, 3, 380–387 (2003).
[3] S.H. Ibbotson, Braz. J. Dermatol., 146, 178-188 (2002).
[4] M.S. Nestor, M.H. Gold, A.N. Kauvar, A.F. Taub, R.G. Geronemus, E.C. Ritvo, M.P. Goldman, D.J. Gilbert, D.F. Richey, T.S. Alster, R.R. Anderson, D.E. Bank, A. Carruthers, J. Carruthers, D.J. Goldberg, C.W. Hanke, N.J. Lowe, D.M. Pariser, D.S. Rigel, P. Robins, J.M. Spencer and B.D. Zelickson, J. Drugs Dermatol., 5, 140-154 (2006).
[5] S.B. Brown and K.J. Mellish, Expert Opin. Pharmacother., 2, 351-361 (2001).
[6] Q. Peng, J. Environ. Pathol. Toxicol. Oncol., 25, 1-6 (2006).
[7] M. Woldemeskel, Vet. Med. Int., 427296 (2012).
[8] M. A. Gertz, Am. J. Hematol., 88, 417 (2013).
[9] C. M. Dobson, Phil. Trans. Royal Soc. B, 356, 133 (2001).
[10] M. Prince, M. Prina, and M. Guerchet, The World Alzheimer Report 2013.
[11] F. Petruzziello, P. Zeppa, L. Catalano, I. Cozzolino, G. Gargiulo, P. Musto, F. D'Auria, V. Liso, R. Rizzi, N. Caruso, C. Califano, E. Piro, M. Musso, V. Bonanno, A. P. Falcone, S. Tafuto, F. D. Raimondo, M. D. Laurentiis, F. Pane, L. Palombini, and B. Rotoli, Annal. Hematol., 89, 469 (2010).
[12] D.R. Booth, M. Sunde, V. Bellotti, C. V. Robinson, W. L. Hutchinson, P. E. Fraser, P. N. Hawkins, C. M. Dobson, S. E. Radford, C. C. F. Blake, and M. B. Pepys, Nature, 385, 787 (1997).
[13] B. Cheng, H. Gong, H. Xiao, R. B. Petersen, L. Zheng, and K. Huang, Biochim. Biophys. Acta, 1830, 4860 (2013).
[14] T. Kawasaki, J. Fujioka, T. Imai, and K. Tsukiyama, The Prot. J., 31, 710 (2012).
[15] T. Kawasaki, T. Imai, and K. Tsukiyama, J. Anal. Sci., Meth. Instrum., 4, 9 (2014).
[16] G. Edwards, R. Logan, M. Copeland, L. Reinisch, J. Davidson, B. Johnson, R. Maciunas, M. Mendenhall, R. Ossoff, J. Tribble, J. Werkhaven and D. O'Day, Nature, 371, 416 (1994).
[17] R.H. Austin, A. Xie, L. van der Meer, B. Redlich, P.-A. Lindgård, H. Frauenfelder and D. Fu, Phys. Rev. Lett., 94, 128101 (2005).
[18] Y. Xiao, M. Guo, P. Zhang, G. Shanmugam, P.L. Polavarapu and M.S. Hutson, Biophys. J., 94, 1359 (2008).
[19] J. Oomens, N. Polfer, D.T. Moore, L. van der Meer, A.G. Marshall, J.R. Eyler, G. Meijer and G. von Helden, Phys. Chem. Chem. Phys., 7, 1345 (2005).
[20] K. Nomaru, M. Kawai, M. Yokoyama, F. Oda, A. Nakayama, H. Koike and H. Kuroda, Nucl. Instrum. Meth. Phys. Res. Sec. A, 445, 379 (2000).
[21] M.I. Apostol, K. Perry and W.K. Surewicz, J. Am. Chem. Soc., 135, 10202 (2013).
[22] A.K. Paravastu, R.D. Leapman, W.-M. Yau and R. Tycko, Proc. Nat. Acad. Sci. USA, 105, 18349 (2008).
[23] H. Itoh-Watanabe, M. Kamihira-Ishijima, N. Javkhlantugs, R. Inoue, Y. Itoh, H. Endo, S. Tuzi, H. Saitô, K. Ueda and A. Naito, Phys. Chem. Chem. Phys., 15, 8890 (2013).
[24] J. Bandekar, Biochim. Biophys. Acta – Prot. Struct. Mol. Enzymol., 1120, 123 (1992).
[25] A. Ahmad, V.N. Uversky, D. Hong and A.L. Fink, J. Biol. Chem., 280, 42669 (2005).
[26] G. Zandomeneghi, M.R.H. Krebs, M.G. McCammon and M. Fändrich, Prot. Sci., 13, 3314 (2004).
[27] L.M. Miller, M.W. Bourassa and R.J. Smith, Biochim. Biophys. Acta, 1828, 2339 (2013).
[28] A.S. Acerbo, G. Lawrence Carr, S. Judex and L.M. Miller, Anal. Chem., 84, 3607 (2012).
[29] R. Gautam, B. Chandrasekar, M. Deobagkar-Lele, S. Rakshit, B.N. Kumar, S. Vinay Umapathy and D. Nandi, PLoS ONE, 7, e45521 (2012).
[30] I. Kakoulli, S.V. Prikhodko, C. Fischer, M. Cilluffo, M. Uribe, H.A. Bechtel, S.C. Fakra and M.A. Marcus, Anal. Chem., 86, 521 (2013).
[31] S. Ling, Z. Qi, D.P. Knight, Y. Huang, L. Huang, H. Zhou, Z. Shao and X. Chen, Biomacromol., 14, 1885 (2013).
[32] L. Chen, H.-Y.N. Holman, Z. Hao, H.A. Bechtel, M.C. Martin, C. Wu and S. Chu, Anal. Chem., 84, 4118 (2012).
[33] T. Yaji, Y. Yamamoto, T. Ohta and S. Kimura, Infra. Phys. Technol., 51, 397 (2008).
[34] M. Reches, Y. Porat and E. Gazit, J. Bio. Chem., 277, 35475 (2002).
[35] K. Tenidis, M. Waldner, J. Bernhagen, W. Fischle, M. Bergmann, M. Weber, M.-L. Merkle, W. Voelter, H. Brunner and A. Kapurniotu, J. Mol. Bio., 295, 1055 (2000).

